A Fast Design Method for Perfect-Reconstruction Uniform Cosine-Modulated Filter Banks

Gerhard Doblinger

***Abstract*—In this correspondence, we present a new and fast design algorithm for perfect-reconstruction (PR), maximally decimated, uniform, cosine-modulated filter banks. Perfect reconstruction is obtained within arithmetic machine precision. The new design does not need numerical optimization routines and is significantly faster than a competing method based on second-order cone programming (SOCP). The proposed design algorithm finds the optimum solution by iteratively solving a quadratic programming problem with linear equality constraints. By a special modification of the basic algorithm, we obtain PR filter banks with high stopband attenuations. In addition, fast convergence is verified by designing PR filter banks with up to 128 channels.**

***Index Terms*—Cosine-modulated filter banks, iterative quadratic programming, perfect-construction filter banks, second-order cone programming.**

I. Introduction

Maximally decimated, uniform, cosine-modulated filter banks play a major role in applications where signals must be processed in subbands. A common example is signal analysis/synthesis with filter banks in MPEG audio coding. In most applications, maximal decimation of subband signals is used to preserve the number of processed samples. Oversampled filter banks need a higher computational cost, but offer advantages for subband processing (e.g., [1]–[3]). Cosine-modulated filter banks provide efficient implementations (e.g., using a discrete cosine transform and polyphase decompositions), and the reduction of the filter bank design to the design of a single prototype filter.

Theory and design of cosine-modulated filter banks are well established and cover a rich set in literature (see e.g., the list of references in [4]). In principle, perfect reconstruction of filter banks requires a solution of nonlinear optimization problems. This leads to computationally intensive design programs, especially for a large number of filter bank channels, and if a high stopband attenuation is required. In addition, design methods based on nonlinear optimization are seriously affected by objective function local minima, and are vulnerable to the selection of a starting solution.

There is a great variety of proposed methods to alleviate the design difficulties. Typically, the perfect reconstruction property is relaxed resulting in near-perfect reconstruction (NPR) filter banks. Efficient NPR design methods are presented in [5]–[10]. NPR designs are sufficient in many practical situations since filter bank amplitude distortions and aliasing errors less than 10^{-3} can easily be obtained. With a PR design, however, we can achieve reconstruction errors within arithmetic machine precision ($\approx 10^{-15}$). The framework of PR design methods leads to optimization problems with nonconvex quadratic constraints solved with nonlinear optimization programs [11]–[13]. Recently, global polynomial optimization techniques have been applied to the design of PR filter banks [14], [15]. Although high-quality filter banks are obtained, this method is currently limited to low-order prototype filters, and to a small number of filter bank channels. Furthermore, its computational complexity is high.

A fast design method of NPR and PR cosine-modulated filter banks based on iterative SOCP is presented in [4]. This technique does not impose a small limit to filter length and number of channels. The PR design of [4] will be compared with our method. We will show that it is possible to avoid numerical optimization programs. As a consequence, the proposed method requires a low computational complexity and needs a significantly lower time to design PR filter banks. Our design method is similar to the iterative procedures presented in [16], [17]. However, we use a different solution strategy and a new approach to avoid convergence to local minima of the objective function.

The paper organization is as follows: In Section II, we briefly summarize the design framework of perfect reconstruction filter banks. The new design algorithm is described in Section III. The design based on SOCP which competes with our method is summarized in Section IV. Representative experimental results and comparison data are discussed in Section V.

II. Cosine-Modulated PR Filter Banks

A maximally decimated filter bank without additional subband processing is composed of M finite impulse response duration (FIR) analysis filters with impulse responses $h_k[n]$, down- and upsampling by factor M of subband signals, and synthesis FIR filters $g_k[n]$. The filter bank impulse responses are obtained by cosine modulation of a lowpass filter as follows:

$$h_k[n] = 2h[n]\cos\left(\frac{\pi}{M}\left(k+\frac{1}{2}\right)\left(n-\frac{D}{2}\right)+(-1)^k\frac{\pi}{4}\right) \quad (1)$$

and

$$g_k[n] = 2h[n]\cos\left(\frac{\pi}{M}\left(k+\frac{1}{2}\right)\left(n-\frac{D}{2}\right)-(-1)^k\frac{\pi}{4}\right), \quad (2)$$

with $k = 0, 1, \ldots, M-1$ and $n = 0, 1, \ldots, N-1$. The filter bank delay is denoted by D, and the prototype lowpass FIR filter impulse response is $h[n]$. In case of a linear phase prototype filter, the delay is $D = N-1$, and the filter bank impulse responses are related by $g_k[n] = h_k[N-1-n], 0 \le k \le M-1, 0 \le n \le N-1$. Therefore, only one set of filter bank coefficients must be stored. In addition, only $\lceil N/2 \rceil$ prototype filter coefficients need to be optimized due to the impulse response symmetry of linear phase filters. In contrast to the linear phase prototype filter $h[n]$, the subband filters $h_k[n]$ and $g_k[n]$ do not exhibit linear phase responses.

Throughout the paper, we assume a linear phase prototype FIR filter with length N being a multiple of $2M$. This is commonly no restriction in applications because $N = 2mM$ leads to efficient filter bank realizations (e.g., [18]).

As derived in [11], the following conditions on the prototype coefficient vector $\mathbf{h}$ must be met to ensure the PR property of the filter bank:

$$\mathbf{h}^T\mathbf{Q}_{l,n}\mathbf{h} = \begin{cases} 0 & 0 \le n \le \frac{N}{2M}-2 \\ \frac{1}{2M} & n = \frac{N}{2M}-1 \end{cases}, \qquad l = 0, 1, \ldots, L_{\max} \quad (3)$$

with $\mathbf{h} = (h[0]\, h[1] \ldots h[N/2-1])^T$, and $L_{\max} = \frac{M}{2}-1$ if M is even, and $L_{\max} = \frac{M-1}{2}$ if M is odd. Matrices $\mathbf{Q}_{l,n}$ are not symmetric but are sparse. The detailed structure of $\mathbf{Q}_{l,n}$ is given in [11].

The PR conditions in (3) guarantee a distortionless and aliasing-free filter bank operation. In addition, the individual subband filters should exhibit a good stopband behavior. In filter bank design, it is common

Manuscript received May 24, 2012; accepted August 06, 2012. Date of publication September 04, 2012; date of current version November 20, 2012. The associate editor coordinating the review of this manuscript and approving it for publication was Prof. Jean-Christophe Pesquet.

The author is with the Institute of Telecommunications, Vienna University of Technology, Vienna 1040, Austria (e-mail: gerhard.doblinger@tuwien.ac.at).

Digital Object Identifier 10.1109/TSP.2012.2217139

practice to minimize the stopband energy of the prototype filter frequency response. As an advantage, such a criterion leads to a quadratic objective function in the resulting optimization problem.

The stopband energy in the frequency band $\theta \in [\theta_s, \pi]$ is given by

$$E_s(\mathbf{h}) = \int_{\theta_s}^{\pi} \left| H(e^{j\theta}) \right|^2 d\theta, \tag{4}$$

with frequency response $H(e^{j\theta}) = \sum_{n=0}^{N-1} h[n] e^{-j\theta n}$ of the prototype filter. Stopband frequency θ_s is typically selected between $\theta_s = \frac{3\pi}{4M}$ and $\theta_s = \frac{4.5\pi}{4M}$. In most applications, we use $\theta_s = \frac{\pi}{M}$. Larger values result in more overlapping of adjacent subband frequency responses, and vice versa. With coefficient vector $\mathbf{h}$, the stop band energy (4) can be written as $E_s(\mathbf{h}) = \mathbf{h}^T \mathbf{P} \mathbf{h}$, and the elements of $\frac{N}{2} \times \frac{N}{2}$ matrix $\mathbf{P}$ can be evaluated in closed form [7], [17].

We can now formulate an optimization problem for the solution of $\mathbf{h}$:

$$\mathbf{h} = \arg\min_{\mathbf{h}} \ \mathbf{h}^T \mathbf{P}\, \mathbf{h} \tag{5}$$

$$\text{s.t.} \quad \mathbf{h}^T \mathbf{Q}_{l,n} \mathbf{h} = c_n, \tag{6}$$

for $l = 0, 1, \ldots, L_{\max}$, $n = 0, 1, \ldots, \left(\frac{N}{2M}\right) - 1$, and with c_n given by the right hand side of (3). There are $N_c = \frac{N}{4}$ equality constraints if M is even, and $N_c = \frac{N}{4M}(M+1)$ for M odd. The quadratic optimization problem in (5) is nonconvex since matrices $\mathbf{Q}_{l,n}$ are not positive definite. Therefore, the constraints in (6) do not form a convex feasible region.

III. Fast Iterative Optimization of PR Filter Banks

The optimization problem (5) can be solved with a nonlinear program like MATLAB® function `fmincon()`. Unfortunately, we observed a high sensitivity in regard to starting solutions, and in most design cases we got NPR filter banks only. Much better solutions are obtained by splitting the optimization task in a sequence of quadratic problems with linearized constraints [16], [17], [19]. Thus, we iteratively solve (5) with a linearization of (6). Each subproblem is convex because matrix $\mathbf{P}$ of the objective function is positive definite.

Let $\mathbf{h}_k$ denote the solution vector at iteration k. We assume that $\mathbf{h}_{k+1}$ at the next iteration differs from $\mathbf{h}_k$ only by a small vector $\boldsymbol{\delta}$, i.e., $\mathbf{h}_{k+1} = \mathbf{h}_k + \boldsymbol{\delta}$, with $\|\boldsymbol{\delta}\|_2 \ll \|\mathbf{h}_k\|_2$ ($\|\cdot\|_2$ denotes L_2 vector norm). Inserting this approximation into the quadratic form in (6) results in

$$\mathbf{h}_{k+1}^T \mathbf{Q}_{l,n}\, \mathbf{h}_{k+1} = \mathbf{h}_k^T \mathbf{Q}_{l,n}\, \mathbf{h}_k + \underbrace{\boldsymbol{\delta}^T \mathbf{Q}_{l,n}\, \boldsymbol{\delta}}_{\text{neglected}} + \underbrace{\mathbf{h}_k^T \left(\mathbf{Q}_{l,n} + \mathbf{Q}_{l,n}^T \right)}_{\mathbf{a}_{l,n}^T(\mathbf{h}_k)} \boldsymbol{\delta}$$

$$\approx \mathbf{h}_k^T \mathbf{Q}_{l,n}\, \mathbf{h}_k + \mathbf{a}_{l,n}^T(\mathbf{h}_k)\, \boldsymbol{\delta}. \tag{7}$$

With (7), the constraints (6) at iteration $k+1$ are approximated by a system of N_c linear equations

$$\mathbf{A}_k \boldsymbol{\delta} = \mathbf{b}_k \tag{8}$$

where $\mathbf{a}_{l,n}^T(\mathbf{h}_k)$ are the rows of $N_c \times \frac{N}{2}$ matrix $\mathbf{A}_k$, and vector $\mathbf{b}_k$ contains $c_n - \mathbf{h}_k^T \mathbf{Q}_{l,n}\, \mathbf{h}_k$ as elements. Note that the system of equations in (8) is underdetermined because of $N_c < \frac{N}{2}$. For each iteration, we now have a convex quadratic programming task with linear equality constraints:

$$\boldsymbol{\delta} = \arg\min_{\boldsymbol{\delta}} \ \left(\mathbf{h}_k^T + \boldsymbol{\delta}^T \right) \mathbf{P} (\mathbf{h}_k + \boldsymbol{\delta}) \tag{9}$$

$$\text{s.t.} \quad \mathbf{A}_k\, \boldsymbol{\delta} = \mathbf{b}_k, \tag{10}$$

for $k = 1, 2, \ldots, K_{\max}$. This problem can be solved in closed form [19]. With the optimized $\boldsymbol{\delta}$, the prototype coefficient vector $\mathbf{h}$ is updated by $\mathbf{h}_{k+1} = \mathbf{h}_k + \boldsymbol{\delta}$. The iteration loop is repeated until the L_2 norm of $\boldsymbol{\delta}$ is less than a lower bound or the maximum number of iterations $K_{\max}$ is reached. It should be noted that (9), (10) do not guarantee that we always get a sufficiently small $\boldsymbol{\delta}$ to achieve convergence. Consequently, we will modify the algorithm later on to fix this problem.

We will discuss two alternative methods to solve (9) with constraints (10): In the first method, we apply a singular value decomposition (SVD) to obtain a particular solution of (10). Alternatively, a QR decomposition is used to solve the underdetermined system of linear equations in (10). With both methods, we eliminate the equality constraints and obtain an unconstrained problem with a quadratic objective function.

The general solution of (10) can be represented by

$$\boldsymbol{\delta} = \boldsymbol{\delta}_p + \mathbf{V}_0 \boldsymbol{\phi}, \tag{11}$$

where $\boldsymbol{\delta}_p$ is a particular solution, and the column vectors of $\mathbf{V}_0$ span the null space of $\mathbf{A}_k$ (i.e., $\mathbf{A}_k \mathbf{V}_0 = \mathbf{0}$). The particular solution may be computed by $\boldsymbol{\delta}_p = \mathbf{A}_k^+ \mathbf{b}_k$ with pseudo inverse $\mathbf{A}_k^+$. Both matrices $\mathbf{V}_0$ and $\mathbf{A}_k^+$ are obtained by the SVD $\mathbf{A}_k = \mathbf{U} \boldsymbol{\Sigma} \mathbf{V}^T$ when only those column vectors of $\mathbf{U}$, $\mathbf{V}$ are taken into account that correspond to singular values greater than a given threshold. There are infinitely many solutions (11) which are parameterized by $\boldsymbol{\phi}$. Inserting the general solution (11) into (9) yields a quadratic cost function of $\boldsymbol{\phi}$. The optimum solution $\boldsymbol{\phi}_{\text{opt}}$ is obtained by setting the gradient of this cost function to zero:

$$\boldsymbol{\phi}_{\text{opt}} = -\left(\mathbf{V}_0^T \mathbf{P} \mathbf{V}_0 \right)^{-1} \mathbf{V}_0^T \mathbf{P} (\mathbf{h}_k + \boldsymbol{\delta}_p). \tag{12}$$

The updated prototype FIR filter coefficient vector is then computed by

$$\mathbf{h}_{k+1} = \mathbf{h}_k + \boldsymbol{\delta}_{\text{opt}} = \mathbf{h}_k + \boldsymbol{\delta}_p + \mathbf{V}_0 \boldsymbol{\phi}_{\text{opt}}, \tag{13}$$

with $\boldsymbol{\delta}_p = \mathbf{A}_k^+ \mathbf{b}_k$.

An alternative solution of the underdetermined system of linear equations in (10) is obtained with a QR decomposition which is computationally more efficient than an SVD. We apply a QR decomposition with column pivoting to the $\frac{N}{2} \times N_c$ matrix $\mathbf{A}_k^T$ [20]:

$$\mathbf{A}_k^T = \mathbf{Q}_k \begin{pmatrix} \mathbf{R}_k \\ \mathbf{0}_k \end{pmatrix} \mathbf{E}_k^T, \tag{14}$$

where $\mathbf{Q}_k$ is an $\frac{N}{2} \times \frac{N}{2}$ orthogonal matrix, $\mathbf{R}_k$ is an $N_1 \times N_c$ upper triangular matrix, $\mathbf{0}_k$ is an $\frac{N}{2} - N_1 \times N_c$ zero matrix. Matrix $\mathbf{E}_k^T$ is an $N_c \times N_c$ permutation matrix used to handle possibly rank-deficient matrices $\mathbf{A}_k^T$. The number of rows N_1 of $\mathbf{R}_k$ is determined by using a small threshold to detect rows with all elements close to zero.

If we define

$$\boldsymbol{\delta}_t = \mathbf{Q}_k^T \boldsymbol{\delta} = \begin{pmatrix} \boldsymbol{\delta}_1 \\ \bar{\boldsymbol{\phi}} \end{pmatrix} \quad \text{and} \quad \mathbf{Q}_k = (\mathbf{Q}_1\ \mathbf{Q}_2), \tag{15}$$

then (10) in combination with (14) leads to

$$\mathbf{R}_k^T \boldsymbol{\delta}_1 = \mathbf{E}_k^T \mathbf{b}_k, \tag{16}$$

where we have used $\mathbf{E}_k \mathbf{E}_k^T = \mathbf{I}$ and $\mathbf{Q}_k \mathbf{Q}_k^T = \mathbf{I}$. Thus, the alternative general solution of (10) is given by

$$\boldsymbol{\delta} = \mathbf{Q}_k \boldsymbol{\delta}_t = (\mathbf{Q}_1\ \mathbf{Q}_2) \begin{pmatrix} \boldsymbol{\delta}_1 \\ \bar{\boldsymbol{\phi}} \end{pmatrix} = \bar{\boldsymbol{\delta}}_p + \mathbf{Q}_2 \bar{\boldsymbol{\phi}}, \tag{17}$$

with $\bar{\boldsymbol{\delta}}_p = \mathbf{Q}_1 \boldsymbol{\delta}_1 = \mathbf{Q}_1 \mathbf{R}_k^{-T} \mathbf{E}_k^T \mathbf{b}_k$ obtained by the solution of (16). General solution (17) can be applied to get an alternative optimum solution

$$\bar{\boldsymbol{\phi}}_{\text{opt}} = -\left(\mathbf{Q}_2^T \mathbf{P} \mathbf{Q}_2 \right)^{-1} \mathbf{Q}_2^T \mathbf{P} (\mathbf{h}_k + \bar{\boldsymbol{\delta}}_p). \tag{18}$$

TABLE I
ALGORITHM TO COMPUTE PROTOTYPE FILTER COEFFICIENT VECTOR $\mathbf{h}$

initialization:	1.	set starting solution of $\mathbf{h} = \mathbf{h}_0$,
	2.	compute $\mathbf{P}$ of stop band energy
	3.	set $K_{\max}$, and error threshold ε
iteration loop:		
$k = 1 \ldots K_{\max}$:	1.	compute $\mathbf{A}_k$, $\mathbf{b}_k$ of (10)
	2.	perform SVD of $\mathbf{A}_k$ or QR-decomp. of $\mathbf{A}_k^T$
	3.	compute $\boldsymbol{\phi}_{\text{opt}}$ with (20)
		(or with (18) modified similar to (20))
	4.	update $\mathbf{h}_k$ with (13) or with (19)
	5.	prematurely exit loop, if $\|\boldsymbol{\delta}\|_2 / \|\mathbf{h}_k\|_2 \leq \varepsilon$

The associated update equation of $\mathbf{h}_k$ is

$$\mathbf{h}_{k+1} = \mathbf{h}_k + \bar{\boldsymbol{\delta}}_{\text{opt}} = \mathbf{h}_k + \bar{\boldsymbol{\delta}}_p + \mathbf{Q}_2 \bar{\boldsymbol{\phi}}_{\text{opt}}. \tag{19}$$

A direct implementation of the proposed algorithm shows convergence problems in cases of filter banks with a moderate number of channels ($M > 6$, typically). In such cases, only an NPR filter bank can be obtained. We found that the presence of $\mathbf{h}_k$ in (12), and (18), respectively, is responsible for a convergence failure. If $\mathbf{h}_k$ is removed in the respective equations, convergence in all cases investigated is ensured. However, removal of $\mathbf{h}_k$ results in a lower stopband attenuation of the filter bank transfer functions. Clearly, this effect is due to the minimization of $\boldsymbol{\delta}^T \mathbf{P} \boldsymbol{\delta}$ instead of $(\mathbf{h}_k^T + \boldsymbol{\delta}^T)\mathbf{P}(\mathbf{h}_k + \boldsymbol{\delta})$ in (9). Fortunately, we can alleviate this problem by a simple modification of the algorithm. During the iteration loop, we check the convergence by observing whether the error norm $\|\boldsymbol{\delta}\|_2 / \|\mathbf{h}_k\|_2$ saturates to a value greater than ε. During the iterations following this event, we modify (12) by removing $\mathbf{h}_k$:

$$\boldsymbol{\phi}_{\text{opt}} = \begin{cases} -\left(\mathbf{V}_0^T \mathbf{P} \mathbf{V}_0\right)^{-1} \mathbf{V}_0^T \mathbf{P}(\mathbf{h}_k + \boldsymbol{\delta}_p) & \text{phase 1} \\ -\left(\mathbf{V}_0^T \mathbf{P} \mathbf{V}_0\right)^{-1} \mathbf{V}_0^T \mathbf{P}\, \boldsymbol{\delta}_p & \text{phase 2} \end{cases}. \tag{20}$$

(phase 1 = before convergence failure is detected, phase 2 = after convergence failure is detected). A similar modification applies to (18). The correct $\boldsymbol{\phi}_{\text{opt}}$ computation during the first iteration phase ensures a high stopband attenuation. Switching to the modified equation ensures convergence to perfect reconstruction in cases where a convergence failure would occur otherwise. This modification is the key point to avoid getting trapped in some local minimum which yields an NPR filter bank only.

The complete algorithm to find $\mathbf{h}$ of the prototype FIR filter is listed in Table I. According to our experiments with a wide range of filter bank specifications, the selection of the starting solution $\mathbf{h}_0$ is not critical. The only requirement is a high stopband attenuation. An FIR filter design with a Kaiser window is sufficient. It is much faster than an equiripple design, especially for large filter lengths N.

IV. ITERATIVE SOCP DESIGN OF PR FILTER BANKS

We compare our design algorithm with a design method proposed in [4]. This method is one of the fastest techniques to design cosine-modulated PR filter banks. Therefore, it is selected for comparison with our design algorithm. The design method in Section IV of [4] uses the convex optimization problem of (9) as a starting point. In contrast to our design method, however, variable $\boldsymbol{\phi}$ of the general solution in (11) $\boldsymbol{\delta} = \boldsymbol{\delta}_p + \mathbf{V}_0 \boldsymbol{\phi}$ is found by the following optimization problem:

$$\boldsymbol{\phi} = \arg\min_{\boldsymbol{\phi}} \left(\mathbf{h}_k + \boldsymbol{\delta}_p + \mathbf{V}_0 \boldsymbol{\phi}\right)^T \mathbf{P} \left(\mathbf{h}_k + \boldsymbol{\delta}_p + \mathbf{V}_0 \boldsymbol{\phi}\right) \tag{21}$$

$$\text{s.t.} \quad \|\boldsymbol{\delta}_p + \mathbf{V}_0 \boldsymbol{\phi}\|_2 \leq \beta. \tag{22}$$

The norm constraint ensures that at each iteration the length of $\boldsymbol{\delta}$ is smaller than a given bound β. This optimization problem is an SOCP which can conveniently be solved with the CVX package [21] and MATLAB®. As discussed in [4], however, convergence to a PR filter bank is obtained only if β is changed during the iteration loop. It is suggested to start with a relatively high value and to decrease β in subsequent iterations. Otherwise, only an NPR filter bank would be obtained. With an iteration-dependent β, convergence can be obtained in a large selection of different filter bank specifications. An expression to modify β during the iterations is not specified in [4]. Our experience show that in certain cases the SOCP will not find a feasible solution if β is decreased too aggressively. However, we always got feasible solutions with the following rule:

$$\beta_{k+1} = \begin{cases} \mu_1 \beta_k & \text{if SOCP solution is feasible at iteration } k \\ \mu_2 \beta_k & \text{otherwise} \end{cases}, \tag{23}$$

with $\mu_1 = 0.5$, and $\mu_2 = 10$, typically. When no feasible SOCP solution $\boldsymbol{\phi}_{\text{opt}}$ is found at iteration k, then in addition to (23) we set $\boldsymbol{\delta}$ to $\boldsymbol{\delta} = \boldsymbol{\delta}_p$ instead to $\boldsymbol{\delta} = \boldsymbol{\delta}_p + \mathbf{V}_0 \boldsymbol{\phi}_{\text{opt}}$ in the update $\mathbf{h}_{k+1} = \mathbf{h}_k + \boldsymbol{\delta}$.

As an alternative to the optimization problem (21), (22), we can apply a QR-factorization instead of an SVD. We recommend to use this method in the experiments due to its faster execution.

V. EXPERIMENTAL RESULTS

In this section, we present typical examples of PR filter bank designs including the convergence behavior of the iterative algorithm with QR decomposition listed in Table I. The same algorithm with SVD works quite similar but requires a larger computation time. In addition, we compare our results with those obtained by the SOCP design of [4]. All experimental data can be reproduced by a MATLAB® program available at the author's homepage [22]. The program has been executed on a PC with Intel® Core™ i7 CPU at 2.67 GHz, running 64 bit Linux MATLAB® version 7.13. The SOCP method has been implemented with CVX version 1.22.

For all filter bank designs shown in this section, we use a transition width between passband and stopband of $\Delta f = \frac{1}{2M}$ (normalized to half the sampling frequency). As a result, adjacent subband transfer functions mainly overlap up to the middle of each subband. Filter banks with even and odd numbers of channels between $M = 2$ and $M = 128$ have been designed. The maximum number of iterations in Table I is set to $K_{\max} = 200$, and an error bound $\varepsilon = 10^{-10}$ is used. A failure of convergence is detected in (20) if the absolute difference of errors (of step 5 in Table I) between two adjacent iterations is less than 10^{-7}, or if $k > 40$. The first case occurs when the error decrease is to slow. The second case covers situations where the error oscillates around a nearly constant value. In case of the SOCP design, a starting value $\beta_0 = 0.5\sqrt{\frac{N}{2}}$ in (23) is applied. As already mentioned, a Kaiser window FIR design is used to obtain a starting solution $\mathbf{h}_0$ of the prototype filter.

The selected examples for comparison cover 7 filter banks with $M \in \{2, 4, 8, 16, 32, 64, 128\}$ channels. The FIR filter length N is chosen to ensure a stopband attenuation of approximately 100 dB. As an example, the individual filter bank channel transfer function magnitudes, overall transfer function magnitude $|T_0(e^{j\theta})|$, and total aliasing transfer function magnitude $|T_a(e^{j\theta})|$ of an $M = 16$ filter bank are plotted in Fig. 1. Frequency parameter $f = \frac{\theta}{\pi}$ is normalized to half the sampling frequency. The total aliasing transfer function magnitude is calculated by

$$\left|T_a\left(e^{j\theta}\right)\right| = \left[\sum_{l=1}^{M-1} \left|T_l\left(e^{j\theta}\right)\right|^2\right]^{\frac{1}{2}} \tag{24}$$

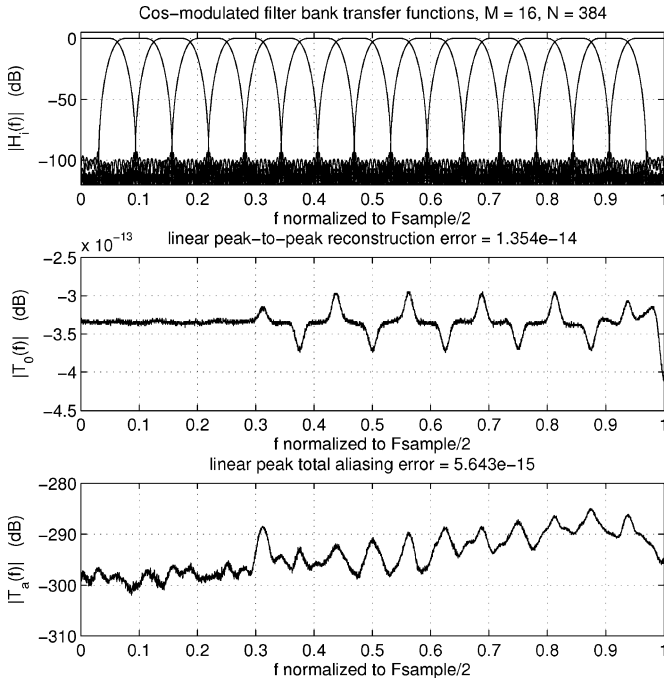

Fig. 1. $M = 16$ channel filter bank, FIR filter length $N = 384$ (channel transfer function magnitudes in dB, overall transfer function magnitude $|T_0(e^{j\theta})|$ in dB, total aliasing transfer function magnitude $|T_a(e^{j\theta})|$ in dB).

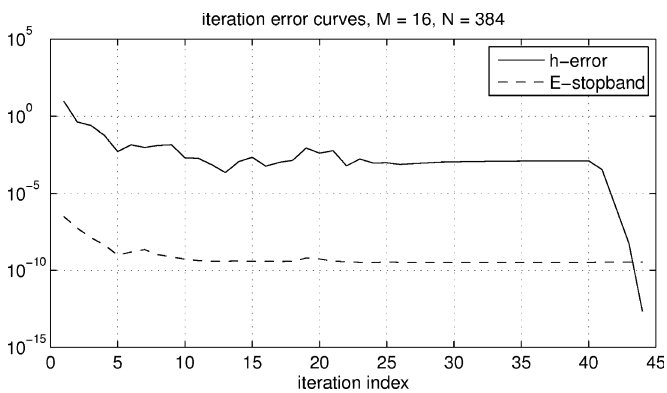

Fig. 2. Impulse response error $\|\boldsymbol{\delta}\|_2/\|\mathbf{h}_k\|_2$ (h-error), and stopband energy (E-stopband) versus iteration index of the $M = 16$ channel PR filter bank.

where $T_l(e^{j\theta})$ are the aliasing transfer functions [4]. As indicated by the diagrams in Fig. 1, both perfect reconstruction within machine precision and a high stopband attenuation are obtained.

The convergence property of our design algorithm is shown in Fig. 2. The drop in the h-error curve at the end of the convergence phase is due to the modification as described by (20). As explained in Section III, both perfect reconstruction and a high stopband attenuation is achieved by this modification.

To compare both design methods, we summarize the main results in Tables II, and III, respectively. In these tables, we list the filter bank reconstruction performances, the final stop band energies, the number of iterations, and the execution time of the design algorithms. Both methods exhibit nearly the same reconstruction and aliasing errors. The stopband energy, however, is larger in case of the SOCP design method. The most prominent difference is observed by comparing the execution times. It is explained by the larger computational cost of SOCP as compared to the demand needed to solve a system of linear equations.

TABLE II
PERFORMANCE OF M CHANNEL PR FILTER BANK DESIGNS PROPOSED IN TABLE I (FIR FILTER LENGTH N, PEAK-TO-PEAK RECONSTRUCTION ERROR $\hat{T}_0$, PEAK TOTAL ALIASING ERROR $\hat{T}_a$, STOPBAND ENERGY E_s, NUMBER OF ITERATIONS N_{iter}, AND EXECUTION TIME T_{exe})

M	N	$\hat{T}_0$ error	$\hat{T}_a$ error	E_s	N_{iter}	T_{exe} (sec)
2	52	2.44e-15	1.02e-15	1.14e-11	21	0.05
4	112	2.22e-15	1.04e-15	3.46e-11	26	0.11
8	224	1.22e-14	3.78e-15	4.49e-11	32	0.27
16	384	1.35e-14	5.64e-15	3.52e-10	44	0.75
32	832	1.86e-14	1.69e-14	1.17e-10	37	1.79
64	1664	3.55e-14	3.65e-14	1.34e-10	42	7.61
128	3328	7.30e-14	8.51e-14	1.14e-10	45	44.12

TABLE III
PERFORMANCE OF M CHANNEL PR FILTER BANK DESIGNS USING THE SOCP METHOD OF [4] (FIR FILTER LENGTH N, PEAK-TO-PEAK RECONSTRUCTION ERROR $\hat{T}_0$, PEAK TOTAL ALIASING ERROR $\hat{T}_a$, STOPBAND ENERGY E_s, NUMBER OF ITERATIONS N_{iter}, AND EXECUTION TIME T_{exe}))

M	N	$\hat{T}_0$ error	$\hat{T}_a$ error	E_s	N_{iter}	T_{exe} (sec)
2	52	2.66e-15	9.49e-16	4.59e-10	23	3.33
4	112	2.22e-15	1.12e-15	2.58e-09	33	6.21
8	224	1.18e-14	3.67e-15	7.37e-11	24	4.57
16	384	1.27e-14	5.31e-15	1.23e-09	38	10.00
32	832	1.82e-14	1.62e-14	2.55e-10	21	14.07
64	1664	3.37e-14	3.53e-14	5.00e-10	31	105.77
128	3328	6.97e-14	8.15e-14	3.10e-10	25	648.02

VI. CONCLUSION

We have presented a new and fast design method for maximally decimated, uniform, cosine-modulated PR filter banks. Perfect reconstruction within machine precision is achieved for all filter bank specifications investigated. The design algorithm avoids numerical optimization routines and is faster than algorithms based on SOCP. Our algorithm iteratively solves a quadratic programming problem with linear equality constraints. The computational complexity per iteration is determined by the need of a QR decomposition (or SVD alternatively), and linear equation solving. A special modification of the straight forward solution ensures convergence to PR filter banks with high stopband attenuations. Although a theoretical convergence proof is currently not available, both algorithms deliver high-quality PR filter banks after some ten iterations.

REFERENCES

[1] H. Bölcskei and F. Hlawatsch, "Oversampled cosine modulated filter banks with perfect reconstruction," *IEEE Trans. Circuits Syst. II*, vol. 45, pp. 1057–1071, Aug. 1998.

[2] L. Gan and K.-K. Ma, "Oversampled linear-phase perfect reconstruction filter banks: Theory, lattice structure and parameterization," *IEEE Trans. Signal Process.*, vol. 51, pp. 744–759, Mar. 2003.

[3] J. Gauthier, L. Duval, and J.-C. Pesquet, "Optimization of synthesis oversampled complex filter banks," *IEEE Trans. Signal Process.*, vol. 57, pp. 3827–3843, Oct. 2009.

[4] W.-S. Lu, T. Saramäki, and R. Bregović, "Design of practically perfect-reconstruction cosine-modulated filter banks: A second-order cone programming approach," *IEEE Trans. Circuits Syst. I*, vol. 51, pp. 552–563, Mar. 2004.

[5] C. Chen and J. Lee, "Design of quadrature mirror filters with linear phase in the frequency domain," *IEEE Trans. Circuits Syst. II*, vol. 39, pp. 593–605, Sep. 1992.

[6] C. D. Creusere and S. K. Mitra, "A simple method for designing high-quality prototype filters for M-band pseudo QMF banks," *IEEE Trans. Signal Process.*, vol. 43, pp. 1005–1007, Apr. 1995.
[7] H. Xu, W.-S. Lu, and A. Antoninou, "Efficient iterative design method for cosine-modulated QMF banks," *IEEE Trans. Signal Process.*, vol. 44, pp. 1657–1668, Jul. 1996.
[8] Y. P. Lin and P. P. Vaidyanathan, "A Kaiser window approach for the design of prototype filters of cosine modulated filterbanks," *IEEE Signal Process. Lett.*, vol. 5, pp. 132–134, Jun. 1998.
[9] M. F. Furtado, Jr., P. S. R. Diniz, and S. L. Netta, "Numerically efficient optimal design of cosine-modulated filter banks with peak-constrained least-squares behavior," *IEEE Trans. Circuits Syst. I*, vol. 52, pp. 597–608, Mar. 2005.
[10] H. H. Kha and T. Q. Nguyen, "Efficient design of cosine-modulated filter banks via convex optimization," *IEEE Trans. Signal Process.*, vol. 57, pp. 966–976, Mar. 2009.
[11] T. Q. Nguyen, "Digital filter bank design quadratic-constrained formulation," *IEEE Trans. Signal Process.*, vol. 43, pp. 2103–2108, Sep. 1995.
[12] P. N. Heller, T. Karp, and T. Q. Nguyen, "A general formulation of modulated filter banks," *IEEE Trans. Signal Process.*, vol. 47, pp. 986–1002, Apr. 1999.
[13] T. Karp and N. J. Fliege, "Modified DFT filter banks with perfect reconstruction," *IEEE Trans. Circuits Syst. II*, vol. 46, pp. 1404–1414, Nov. 1999.
[14] J. Yan and W.-S. Lu, "Towards global design of orthogonal filter banks and wavelets," *Can. J. Elect. Comput. Eng.*, vol. 34, pp. 145–151, Fall 2009.
[15] J. Yan and W.-S. Lu, "Global design of perfect-reconstruction orthogonal cosine-modulated filter banks," in *Proc. CCECE*, Calgary, AB, Canada, May 2010, pp. 1–4.
[16] Y.-T. Fong and C.-W. Kok, "Iterative least squares design of DC-leakage free paraunitary cosine modulated filter banks," *IEEE Trans. Circuits Syst. II*, vol. 50, pp. 238–243, May 2003.
[17] Z. Zhang, "Design of cosine modulated filter banks using iterative Lagrange multiplier method," in *Proc. IEEE Int. Symp. Microw., Antenna, Propag., EMC Technol. for Wireless Communications. (MAPE)*, Aug. 8–12, 2005, vol. 1, pp. 157–160.
[18] J. H. Rothweiler, "Polyphase quadrature filters—A new subband coding technique," in *Proc. IEEE Int. Conf. Acoust., Speech, Signal Process. (ICASSP)*, Boston, MA, 1987, pp. 1280–1283.
[19] A. Antoninou and W.-S. Lu, *Practical Optimization—Algorithms and Engineering Applications*. New York: Springer, 2007.
[20] G. Golub and C. F. van Loan, *Matrix Computations*. Baltimore, MD: The Johns Hopkins Univ. Press, 1985.
[21] M. Grant and S. Boyd, Cvx Users' Guide. ver. 1.22, Jan. 2012 [Online]. Available: http://cvxr.com/cvx/
[22] MATLAB® program prfib.m,. Feb. 2012 [Online]. Available: www.nt.tuwien.ac.at/staff/gerhard-doblinger/

Commutative Anisotropic Convolution on the 2-Sphere

Parastoo Sadeghi, Rodney A. Kennedy, and Zubair Khalid

***Abstract*—We develop a new type of convolution between two signals on the 2-sphere. This is the first type of convolution on the 2-sphere which is commutative. Two other advantages, in comparison with existing definitions in the literature, are that 1) the new convolution admits anisotropic filters and signals and 2) the domain of the output remains on the sphere. Therefore, the new convolution well emulates the conventional Euclidean convolution. In addition to providing the new definition of convolution and discussing its properties, we provide the spectral analysis of the convolution output. This convolutional framework can be useful in filtering applications for signals defined on the 2-sphere.**

***Index Terms*—Commutative convolution, convolution, spherical harmonics, 2-sphere (unit sphere).**

I. Introduction

In many applications in physical sciences and engineering, the domain of signals under investigation is defined on the 2-sphere, $\mathbb{S}^2$. These applications include geophysics [1], cosmology [2], electromagnetic inverse problems [3], medical imaging [4] and wireless communication systems [5]. It is often required that signal processing techniques developed for the Euclidean domain be extended and tailored in non-trivial ways so that they are suitable and well-defined for the spherical domain. One important signal processing tool is convolution between two signals defined on the 2-sphere, which is fundamental for filtering applications.

It turns out that an analog of the Euclidean-domain convolution on the 2-sphere does not exist yet in the literature. While there are various formulations [4], [6]–[10], they lack some desired or expected properties as we explain below.

One well-known and widely-used definition for convolution on the 2-sphere appears in [6], which has been generalized for the n-sphere and applied for estimation of probability density function in [11]. The advantage of this convolution is that it results in a simple multiplication of the spectral (spherical harmonic) coefficients of the signal and filter in the Fourier domain. However, the convolution involves full rotation of the filter by all independent Euler angles which includes an extra averaging over the first rotation about the $z-$ axis. This is presumably done to ensure that the output domain of convolution is $\mathbb{S}^2$, but it results in smoothing the filter by projecting it into the subspace of azimuthally symmetric signals. Consequently, this convolution becomes identical to a simpler isotropic convolution [9], [10] as shown in [12]. In contrast to conventional convolution in the Euclidean domain, due to excessive smoothing, convolution in [6], [9], [10] is not commutative and discards information.

Another definition of convolution for signals on the 2-sphere can be found in [4], [7] and has been referred to as directional correlation in

Manuscript received March 22, 2012; revised June 27, 2012; accepted August 28, 2012. Date of publication September 06, 2012; date of current version November 20, 2012. The associate editor coordinating the review of this manuscript and approving it for publication was Dr. Andrzej Cichocki. This work was supported under the Australian Research Council's Discovery Projects funding scheme (project no. DP1094350).

The authors are with the Research School of Engineering, College of Engineering and Computer Science, The Australian National University, Canberra, Australia (e-mail: parastoo.sadeghi@anu.edu.au; rodney.kennedy@anu.edu.au; zubair.khalid@anu.edu.au).

Color versions of one or more of the figures in this paper are available online at http://ieeexplore.ieee.org.

Digital Object Identifier 10.1109/TSP.2012.2217337